

# Optimization of source-detector separation for enhanced spatially resolved fluorescence from epithelial layer

Nemichand<sup>a</sup>, Shivam Shukla<sup>b</sup>, Pankaj Singh<sup>c</sup>, and Asima Pradhan<sup>a,b</sup>

<sup>a</sup>Department of Physics, Indian Institute of Technology, Kanpur (U.P.), India

<sup>b</sup>Center for Lasers and Photonics, Indian Institute of Technology, Kanpur (U.P.), India

<sup>c</sup>Department of Physics, Allahabad Degree College, Prayagraj (U.P.), India

## ABSTRACT

Epithelial cancers, constituting the majority of human cancer cases, can be identified by alterations in the biochemical and morphological characteristics of the thin epithelial layer (ranging from 100  $\mu\text{m}$  to 500  $\mu\text{m}$ ), serving as an initial indication of the disease. Many researchers have utilised spatially resolved fiber optic probes and fluorescence spectroscopy technique to detect subtle variations in the optical properties of the epithelium layer of tissue. This study explores the impact of the incident and different collection configurations on epithelium layer sensitivity for spatially resolved fluorescence. Monte Carlo simulation reveals that a fiber probe with illumination-collection at 45-degree beveled angle in parallel configuration provides maximum fluorescence from the epithelium layer. This configuration is suitable for both *in vitro* and *in vivo* settings for epithelial precancer diagnosis. The efficacy of the 45-degree beveled angle fiber probe for measuring spatially resolved sensitivity has also been validated experimentally using two layer solid tissue-mimicking phantoms which demonstrates strong agreement with the results generated from Monte Carlo simulation. These findings suggest that employing an optimum source detector configuration enables the collection of enhanced spatially resolved fluorescence from the epithelium layer.

**Keywords:** Monte Carlo simulation, Epithelial cancer, Spatially resolved fluorescence, Fiber optic probe, Tissue mimicking phantom

## 1. INTRODUCTION

Monte Carlo simulations have been explored by various researchers for simulating light transport in biological tissue to estimate the diffuse reflectance, internal absorption, transmission at the boundaries, and fluorescence from the medium.<sup>1–3</sup> Monte Carlo multi-layer (MCML) simulation program proposed by Wang and Jacques et al. can be used for various light-tissue interactions in different layers.<sup>4</sup> The optimized fiber-optic probe designs that are suitable for *in-vivo* clinical settings can be decided by Monte Carlo-based models, which can also accurately characterize photon propagation in multilayered tissue geometries.

The optical, chemical, and structural properties of tissue change with the growth of cancer. In epithelial cancer, the changes start in the epithelium-stroma inter layer and progress to the entire epithelium layer with disease progression. At the highest grade of disease, these changes invade the stromal layer and break the connective tissue cells there. Capturing these changes would help in differentiating the normal and diseased tissues. Optical diagnostic methods have shown the potential for precancer detection using diffuse reflectance spectroscopy, fluorescence spectroscopy, optical imaging, high-resolution microscopy, Mueller polarimetry, and optical coherence tomography.<sup>5–8</sup> These optical techniques have the ability to provide minimally invasive, radiation-free, and rapid diagnosis tools for screening and disease diagnosis.

Fluorescence spectroscopy, especially, has been a widely used tool for rapid, minimally invasive, and quantitative probing of the biochemical and morphological changes in precancer and cancer tissues.<sup>9–11</sup> Fluorescence spectroscopy was used by Alfano R.R. et al. to distinguish between malignant and healthy breast tissue.<sup>12</sup> Maya

---

Further author information: (Send correspondence to A.P.)

A.P.: E-mail: asima@iitk.ac.in, Telephone: 0512-259-7691

Nemichand: E-mail: nemic@iitk.ac.in, Telephone: 0512-259-7971

S et al. used spatially resolved fluorescence to diagnose breast tissue using changes in optical parameters with disease progression.<sup>13</sup> Using an intrinsic fluorescence-based investigation, B.L. Meena and colleagues distinguished between normal and diseased cervical tissue.<sup>14</sup> Kumar P. et al. compared fluorescence and Stokes shift spectroscopy to detect oral precancerous lesions using human saliva as a diagnostic medium.<sup>15</sup> Fibre probes are usually employed for photon illumination and spatially resolved collection on the tissue surface using the diffuse reflectance and fluorescence measurements. Fiber probe geometry is typically tailored based on the tissue being studied and the efficient acquisition of valuable information. Zhu et al. analyzed the sensitivity of fiber probes using depth-resolved fluorescence for a single fiber and a multifiber, with both illumination and collection being normal to the surface.<sup>16</sup> Pfefer et al. showed the effect of fiber probe geometry on depth-resolved fluorescence for a single layer in low and high-attenuation media.<sup>17</sup> Malignant and normal tissue can be discriminated by choosing suitable fiber-optic probe geometries. In diffuse reflectance, the Oblique illumination and Oblique collection in parallel configuration (O-O-P) fiber-optic probe shows the ability to efficiently collect epithelial diffuse photons, but source detector separation (SDS) limits the photon collection region.<sup>19</sup> Therefore, a different approach to obtain the crucial epithelial signature is required. Additionally, fluorescence can be used to capture variations in fluorophore concentration with disease progression.

In this study, Monte-Carlo simulations have been applied to model the propagation of illumination light, emitted fluorescence light from the tissue, and the accumulation of light within the tissue. Certain fiber probe geometries have been investigated to evaluate the influence of fiber probe geometry on the collection of spatially resolved fluorescence from the epithelial tissue. Different fiber probe geometries has been analysed using depth-resolved fluorescence to obtain an optimized fiber probe geometry that efficiently collects epithelial fluorescence for the diagnosis of epithelial precancer. It is found that the O-O-P fiber probe geometry is efficient in collecting epithelial fluorescence which was also the optimal configuration for diffuse reflectance measurements.<sup>19</sup> The spatially resolved epithelium sensitivity shows that in the fiber beveled direction, a region with high epithelial sensitivity is observed at high source-detector separation which enables efficient collection of fluorescence photons.

## 2. MATERIALS AND METHODS

### 2.1 Optical properties of the tissue mimicking medium

A bi-layer tissue mimicking medium of the epithelial tissue with different illumination-collection configurations, as shown in Figure 1, has been considered for the propagation of elastically scattered as well as fluorescence photons in the Monte Carlo simulation. The epithelial tissue consists of a  $300\ \mu\text{m}$  epithelial layer at the top and a semi-infinite stroma layer at the bottom. Optical parameters of the tissue-mimicking phantom for simulation at excitation (405 nm) and emission wavelengths (530 nm) are listed in Table 1. The fluorescence efficiency for the epithelium and stroma layer has been taken to be 1. Both layers have a refractive index of 1.4, and the refractive index of the core of the fiber (i.e., the medium just above the tissue surface) has been chosen to be 1.5. The half acceptance angle of fiber is approximately  $9^\circ$ , corresponding to the numerical aperture (NA) of 0.22, and the diameter of the fiber is  $100\ \mu\text{m}$ .

### 2.2 Monte Carlo fluorescence simulation

MCML program written in C language simulates the propagation of light in a multi-layered medium. However, the reported MCML program is restricted for normal illumination; hence all physical quantities are stored in cylindrical grids. The oblique illumination collection geometry breaks the cylindrical symmetry, so necessary modifications in the program have been implemented to store physical quantities on the surface in two-dimensional square grids and within the medium in three-dimensional cubical grids, respectively. We have used two distinct subroutines to simulate light propagation within the tissue. The excitation subroutine includes the illumination of the medium by light at the excitation wavelength and light absorption by a fluorophore in the cubical grids of the dimension  $0.001\ \text{cm}$ . In the emission subroutine, isotropically generated fluorescence photons from the center of the cubical grid propagate within the medium according to the optical properties of the medium at the emission wavelength. The fluorescence photon generation depends on the absorption of excitation light and fluorescence efficiency.

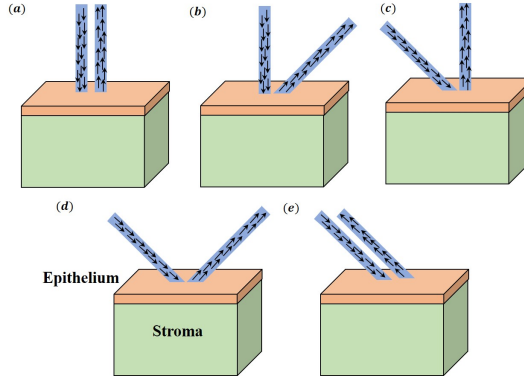


Figure 1. Different fiber probe geometries where a, b, c, d, e represent Normal illumination-Normal collection(N-N), Normal-Oblique(N-O), Oblique-Normal(O-N), Oblique-Oblique-Opposite(O-O-O), and Oblique-Oblique-Parallel(O-O-P) configuration.

### 2.3 Phantom preparation and Experimental setup

We have utilized a multi-fiber probe consisting of 77 fibers beveled at  $45^\circ$  from the fiber axis, and the detailed specification of the probe can be found in previous publications from our research group.<sup>19, 20</sup> Different combinations for the source and detector were identified at different source-detector separations (SDS) along the beveled direction of the fiber probe. We have chosen 10 fiber combinations to obtain the spatially resolved fluorescence starting from the source position up to  $0.1\text{ cm}$  along the beveled direction(+ X-axis). A fiber-coupled  $405\text{ nm}$  diode laser has been used as the incident light source and, the fluorescence spectrum is measured using a USB2000 Ocean Optics spectrometer.

A tissue-mimicking phantom is prepared using Nigrosin dye as an absorber, Intralipid as a scatter, Flavin Adenine Dinucleotide (FAD) as a fluorophore, and, an aqueous solution of Agar powder as a medium. Two bi-layer phantoms have been used to collect epithelial and stromal layer fluorescence. The total absorption and scattering coefficient of the layers in both phantoms is kept same at the excitation wavelength. The first bi-layer phantom has FAD only in the epithelial layer so any fluorescence detected from this phantom implies that it is from the epithelial layer. Second phantom has FAD only in stroma layer implying that fluorescence collected will be from stroma layer. The fluorescence is measured at the emission peak wavelength ( $530\text{ nm}$ ) of FAD for both phantoms at 10 different SDS. The laser power for excitation light is kept constant for all the measurements.

## 3. RESULTS AND DISCUSSION

### 3.1 Optimised fiber probe geometry

For epithelium precancer diagnosis, one would be interested in obtaining a fiber illumination-collection configuration that collects maximum fluorescence from the top layer. We have simulated all five possible illumination-collection fiber configurations for depth-resolved fluorescence (DRF) to obtain the optimised fiber probe configuration. Figure 2(a) shows the normalized depth resolved fluorescence for different geometries in which the O-O-O fiber probe geometry has the least attenuation length(a depth into the medium from the surface where the depth-resolved fluorescence falls to  $1/e$  of its maximum value.), but this configuration is inapplicable for in-vivo applications. Thus, the O-O-P fiber probe geometry(with the second lowest attenuation length) is found to be an efficient fiber probe geometry and is a suitable choice for both in-vitro and in-vivo applications. The attenuation length for the different geometries is shown in Table 2.

The normalized depth resolved fluorescence versus depth plot shown in Figure 2(b) for beveled angles ( $0^\circ, 15^\circ, 30^\circ, 45^\circ$ , and  $60^\circ$ ) deduce that the attenuation length is least for the  $60^\circ$  beveled angle. However, the total fluorescence collected on the surface is only 40% of the maximum fluorescence(Figure 2(c)). Thus, the  $45^\circ$  beveled fiber illumination collection configuration is optimized geometry for collection of maximum depth resolved fluorescence

from epithelial layer.

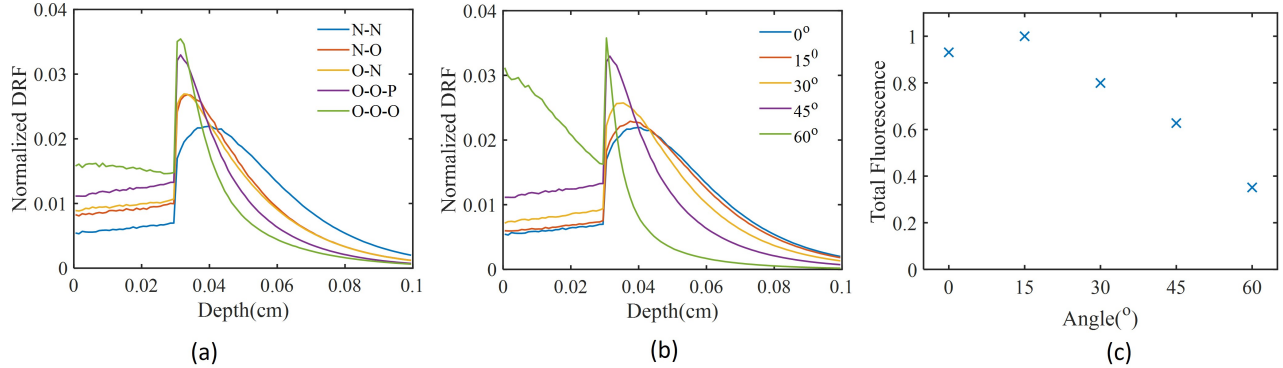


Figure 2. (a) Normalized depth-resolved fluorescence for different fiber probe geometries (O-O-P, O-N, O-O-O, N-N, and N-O). (b) Normalized depth-resolved fluorescence for different beveled angles ( $0^\circ$ ,  $15^\circ$ ,  $30^\circ$ ,  $45^\circ$ , and  $60^\circ$ ) for O-O-P fiber probe geometry. (c) Total fluorescence for fiber beveled angles ( $0^\circ$ ,  $15^\circ$ ,  $30^\circ$ ,  $45^\circ$ , and  $60^\circ$ ) for O-O-P fiber probe geometry.

Table 1. Optical properties of tissue-mimicking turbid medium used for Monte Carlo simulation.<sup>18</sup> ( $n$ -refractive index of layer,  $\mu_a$  - absorption coefficient,  $\mu_s$  - scattering coefficient,  $g$  -anisotropy, and  $d$  -layer thickness.)

Layer	$n$	Excitation		Emission		$g$	$d(cm)$
		$\mu_a(cm^{-1})$	$\mu_s(cm^{-1})$	$\mu_a(cm^{-1})$	$\mu_s(cm^{-1})$		
Epithelial	1.4	3.14	41.7	1.75	30.5	0.95	0.03
Stroma	1.4	7.08	275.7	3.13	209.6	0.88	2.0

Table 2. Attenuation length for different fiber probe geometries and O-O-P at different beveled angles

Fiber probe geometry	attenuation length(cm)	for O-O-P fiber probe geometry	
		Angle(°)	attenuation length(cm)
N-N	0.069	0	0.069
N-O	0.056	15	0.068
O-N	0.055	30	0.059
O-O-P	0.047	45	0.047
O-O-O	0.042	60	0.036

### 3.2 Spatially resolved fluorescence

In fluorescence, the epithelial sensitivity is defined as the fraction of collected fluorescence photons originating from the epithelial layer, which mainly indicates the changes in the fluorescence concentration with disease progression. The fiber probe with high epithelium sensitivity collects a high fraction of epithelium photons, making it more sensitive to epithelial changes. We have simulated epithelium sensitivity for fluorescence for a  $45^\circ$  beveled fiber illumination-collection configuration(O-O-P), as shown in Figure 3.

From the figure, it can be clearly seen that the epithelial sensitivity along the Y axis is symmetric and monotonically decreases with increasing SDS. Along the + X-axis, the sensitivity decreases rapidly up to 0.025 cm SDS, after that it starts increasing, and takes a maximum value at SDS 0.07 cm. Further, we experimentally measured spatially resolved sensitivity along the direction of the beveled fiber(+ X-axis) to verify the enhanced epithelial sensitivity region. From the experimental results, we have observed a similar pattern of the epithelial sensitivity along the + X axis as depicted in the simulation result. It proves that this O-O-P geometry based fiber

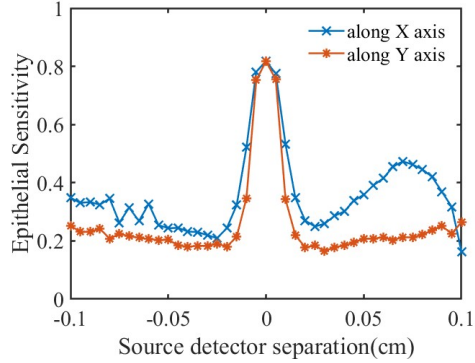


Figure 3. Spatially resolved fluorescence epithelial sensitivity along the fiber beveled direction(X-axis) and normal to the beveled direction(Y-axis) simulated using Monte Carlo fluorescence simulation.

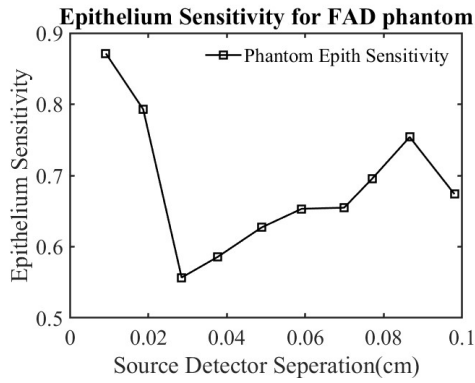


Figure 4. Experimentally measured epithelium sensitivity for bi-layer tissue mimicking FAD phantom along the fiber beveled direction (+ X-axis).

optic probe can efficiently collect epithelial fluorescence even at large source-detector separation which makes this fiber probe configuration suitable for precancer diagnosis.

#### 4. CONCLUSION

Monte Carlo simulation can be used to model light propagation in turbid media. In the present study, we have investigated five different fiber probe configurations to obtain an optimised geometry for the collection of enhanced spatially resolved fluorescence from epithelial layer. Our simulation results have shown that the 45 degree beveled O-O-P fiber probe geometry collects maximum fluorescence from the epithelial layer and it is also suitable for in-vitro and in-vivo applications. Experimental validation of the epithelial sensitivity for O-O-P geometry suggests that this geometry is efficient in capturing epithelial layer changes even at the large source detector separations.

#### 4.1 Acknowledgments

Nemichand would like to acknowledge IIT Kanpur for the Institute fellowship for research work.

#### REFERENCES

- [1] Changfang Zhu, Gregory M. Palmer, Tara M. Breslin M.D., Josephine M. Harter M.D., Nirmala Ramanujam, "Diagnosis of breast cancer using fluorescence and diffuse reflectance spectroscopy: a Monte-Carlo-model-based approach," J. Biomed. Opt. 13(3) 034015 (1 May 2008)

- [2] George Zonios and Aikaterini Dimou, "Modeling diffuse reflectance from homogeneous semi-infinite turbid media for biological tissue applications: a Monte Carlo study," *Biomed. Opt. Express* 2, 3284-3294 (2011)
- [3] Hassan, N.I., Hassan, Y.M., Mustafa, T.A. et al. Modeling optical fluence and diffuse reflectance distribution in normal and cancerous breast tissues exposed to planar and Gaussian NIR beam shapes using Monte Carlo simulation. *Lasers Med Sci* 38, 96 (2023).
- [4] Wang, L.; Jacques, S.L.; Zheng, L. MCML—Monte Carlo modeling of light transport in multi-layered tissues. *Comput. Methods Progr. Biomed.* 1995, 47, 131–146.
- [5] Singh, P., Sahoo, G. R., and Pradhan, A., "Spatio-temporal map for early cancer detection: Proof of concept," *Journal of biophotonics* 11(8), e201700181 (2018).
- [6] Sahoo, G. R., Shukla, S., and Pradhan, A., "Wavelet leader based multifractal analysis of phase contrast images for cervical pre-cancer detection," in [European Conference on Biomedical Optics ], 11076 60, Optical Society of America (2019).
- [7] Bergmeir, C., Silvente, M. G., and Ben 'itez, J. M., "Segmentation of cervical cell nuclei in high-resolution microscopic images: A new algorithm and a web-based software framework," *Computer methods and programs in biomedicine* 107(3), 497–512 (2012).
- [8] Feng, S., Lin, D., Lin, J., Li, B., Huang, Z., Chen, G., Zhang, W., Wang, L., Pan, J., Chen, R., et al., "Blood plasma surface-enhanced raman spectroscopy for non-invasive optical detection of cervical cancer," *Analyst* 138(14), 3967–3974 (2013).
- [9] Chance, B., Schoener, B., Oshino, R., Itshak, F., and Nakase, Y., "Oxidation-reduction ratio studies of mitochondria in freeze-trapped samples. nadh and flavoprotein fluorescence signals.," *Journal of Biological Chemistry* 254(11), 4764–4771 (1979).
- [10] Alfano, R., Tata, D., Cordero, J., Tomashevsky, P., Longo, F., and Alfano, M., "Laser induced fluorescence spectroscopy from native cancerous and normal tissue," *IEEE Journal of Quantum Electronics* 20(12), 1507–1511 (1984).
- [11] Richards-Kortum, R., Rava, R., Petras, R., Fitzmaurice, M., Sivak, M., and Feld, M., "Spectroscopic diagnosis of colonic dysplasia," *Photochemistry and photobiology* 53(6), 777–786 (1991).
- [12] Alfano, R., Tang, G., Pradhan, A., Lam, W., Choy, D., and Opher, E., "Fluorescence spectra from cancerous and normal human breast and lung tissues," *IEEE Journal of Quantum Electronics* 23(10), 1806–1811 (1987).
- [13] Maya S. Nair, Nirmalya Ghosh, Narisetty Sundar Raju, and Asima Pradhan, "Determination of optical parameters of human breast tissue from spatially resolved fluorescence: a diffusion theory model," *Appl. Opt.* 41, 4024-4035 (2002)
- [14] Meena, B. L., Singh, P., Sah, A. N., Pandey, K., Agarwal, A., Pantola, C., and Pradhan, A., "Intrinsic fluorescence for cervical precancer detection using polarized light based in-house fabricated portable device," *Journal of biomedical optics* 23(1), 015005 (2018).
- [15] Kumar, P., Singh, A., Kanaujia, S. K., and Pradhan, A., "Human saliva for oral precancer detection: a comparison of fluorescence stokes shift spectroscopy," *Journal of fluorescence* 28(1), 419–426 (2018).
- [16] Zhu, C., Liu, Q., Ramanujam, N. (2003). Effect of fiber optic probe geometry on depth-resolved fluorescence measurements from epithelial tissues: a Monte Carlo simulation. *Journal of Biomedical Optics*, 8(2), 237-247.
- [17] J. Pfefer, A. Agrawal, and R. Drezek, "Simulation of Oblique-Incidence Probe Geometries for Depth-Resolved Fluorescence Spectroscopy," in *Diagnostic Optical Spectroscopy in Biomedicine III*, A. Mycek, ed., Vol. 5862 of Proc. SPIE (Optica Publishing Group, 2005), paper ThB5.
- [18] Dizem Arifler, Calum E. MacAulay, Michelle Follen, Rebecca R. Richards-Kortum, "Spatially resolved reflectance spectroscopy for diagnosis of cervical precancer: Monte Carlo modeling and comparison to clinical measurements," *J. Biomed. Opt.* 11(6) 064027 (1 November 2006) <https://doi.org/10.1117/1.2398932>
- [19] Singh, P.; Pandey, P.; Shukla, S.; Naik, N.; Pradhan, A. Modelling, Design and Validation of Spatially Resolved Reflectance Based Fiber Optic Probe for Epithelial Precancer Diagnostics. *Appl. Sci.* 2020, 10, 8836.
- [20] Shivam Shukla, Pankaj Singh, Prabodh Kumar Pandey, Asima Pradhan, "Extraction of thickness and fluorophore concentration of the upper layer in a two-layered solid phantom using spatially resolved fluorescence spectroscopy," *Proc. SPIE* 11363, *Tissue Optics and Photonics*, 113631L (2 April 2020);<https://doi.org/10.1117/12.2552978>